RSC Advances

ROYAL SOCIETY OF CHEMISTRY

www.rsc.org/advances

Journal Name

ARTICLE

A novel magnetic fluorescent chemosensor for Cu^{2+} based on self-assembled systems of azobenzene and α-cyclodextrin

Received 00th January 20xx,
Accepted 00th January 20xx

DOI: 10.1039/x0xx00000x

www.rsc.org/

Yue Zhang[a], Qiang Li[a], Jing Guo[a], Yaoxian Li[a], Qingbiao Yang*[a],Jianshi Du**[b]

A novel fluorescent and colorimetric chemosensor for Cu^{2+} has been designed and fabricated. Using host-guest interactions to construct the inclusion complex magnetic nanoparticles (IFIC MNPs) from Azobenzene-modified rhodamine 6G and α-cyclodextrin-modified Fe_3O_4@SiO_2. A selective 'turn-on' type fluorescent enhancements and an apparent colour change from colourless to yellow-green with Cu^{2+} ions in the experiment of fluorescence and light yellow to pink in UV-visible spectra can be achieved. Good selectivity and sensitivity for Cu^{2+} of the IFIC MNPs can be gained with a detecting limit of 2.5×10^{-7} M in MeCN/H_2O=1:1. Further more, the IFIC magnetic nanoparticles can be seperated and recycled easily by a magnet due to its superparamagnetism.

Introduction

Among the heavy metal ions copper is significant pollutant due to its widespread applications in the field of industry.[1,2] Pathology investigations have also shown that the abnormal concentration of copper ions in the nervous system can cause diseases such as Alzheimer's and Parkinson's.[3] Although there have been many articles reported,[4-7] it is still intriguing to develop new methodologies for the detecting of copper ions in aqueous solutions with both high sensitivity and selectivity.

Recent reports have shown great interests in developing chemosensors based on magnetic nanoparticles. The good dispersibility and strong magnetic responsivity of them indicated potent applications to detection and separation of metal ions.[8,9] These nanoparticles own high surface areas due to its core-shell structures composed of both inorganic and organic components. Recent studies also showed chromogenic or fluorogenic features of these magnetic silica nanoparticles and capacities for fluorescent sensor applications.[10-13]

A fascinating alternative to the preparation of functionalized magnetic chemosensors is using of supramolecular interactions which can be easily tuned by the geometrical complementary of host and guest molecules such as α-cyclodextrin (α-CD) (host) and azobenzene (guest).[14] Being different from the ones which were fabricated through covalent bond, these magnetic nanoparticle-based chemosensors can be used repeatedly. No defects such as fluorophore leaking, thickness control, inner-layer analyte diffusion, poor aqueous solubility and strict reaction conditions have been encountered during the preparation compared with traditional methods.[15] So far, some reports have already put this methodology into use for application in fluorescent self-assembled innermonolayers.[16]

With the inspiration triggered by this neoteric method in mind, we have designed and fabricated a novel magnetic nanoparticle-based chemosensor composed of rhodamine-azobenzene loaded magnetic nanoparticles in this paper. The fluorescent receptor rhodamine-azobenzene has been fastened to the surfaces of MNPs only by the host-guest interactions, and the release is automatically facilitated only by changing the solvent conditions (Scheme 1).[17] Moreover, the response is faster due to the direct exposure of fluorophores fabricated in such a self-assembling way than those packaging in a physical process, and the recycle of the sensing molecules and nanoparticles is facile and effective due to the magnetic nature and host-guest structure of this MNPs. It is promising that ITCRh6G-Azo/Fe_3O_4@SiO_2-α-CD inclusion complex magnetic nanoparticles (IFIC-MNPs) could act as highly selective and sensitive fluorescent and colorimetric sensors for detecting trace Cu^{2+} ions, which can be used repeatedly.

[a] Department of Chemistry, Jilin University, Changchun, 130021 (P. R. China). E-mail address: yangqb@jlu.edu.cn (Q. B. Yang).
[b] Address here. China Japan union hospital, Jilin University, Changchun, 130031 (P. R. China). E-mail address: dujianshi3043@126.com (J. S. Du).
† Electronic Supplementary Information (ESI) available: experimental details, additional spectroscopic data. See DOI: 10.1039/x0xx00000x

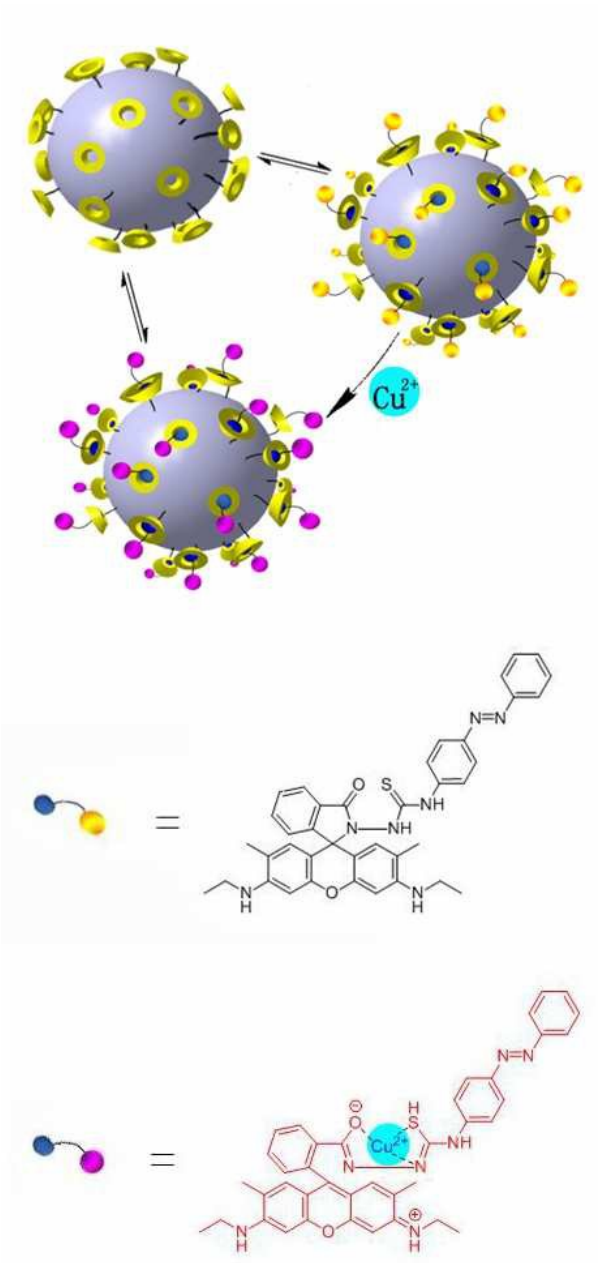

Scheme 1 Chemical and schematic illustration of the preparation of IFIC NMPs sensor for Cu^{2+}.

Experimental

Materials and reagents

Rhodamine 6G (Rh6G), α-cyclodextrin (α-CD), triethylamine and 4-aminoazobenzene were purchased from Sigma-Aldrich. Thionyl chloride, ammonia, tetraethylorthosilicate (TEOS) and hydrazine hydrate were obtained from Alfa Aesar. γ-(2,3-Epoxypropoxy) propytrimethoxysilane (KH-560, 99%) was obtained from Acros Organics. All the reagents and inorganic metal salts with analytical grade (Shanghai Chemical Reagents Co. China) were used without further purification. The solutions of metal ions were prepared from $CaCl_2$, $CoCl_2·6H_2O$, $MgSO_4$, $BaCl_2·2H_2O$, $CdCl_2$, $Mn(NO_3)_2·6H_2O$, $Zn(NO_3)_2·6H_2O$, $NiCl_2·6H_2O$, $HgCl_2$, KCl, $FeCl_3·6H_2O$, $CuCl_2·2H_2O$, $Pb(NO_3)_2$ respectively, and were dissolved in deionized water. Aqueous Tris-HCl (0.05 mol L^{-1}) solution was used as buffer to keep pH value (pH=7.20), and to maintain the ionic strength of all solutions in experiments.

Apparatus

^1H and ^{13}C NMR spectra were measured on a Varian Mercury-300BB NMR spectrometer. The pH values of the test solutions were measured with a glass electrode connected to a Mettler-Toledo Instruments DELTA 320 pH meter (Shanghai, China) and adjusted if necessary. The morphology of the nanoparticles was observed on a Hitachi SU8020 scanning electron microscope. The magnetic hysteresis loops were measured on a Quantum Design SQUID-MPMS-XL magnetic property measurement system. FTIR spectra of the products were recorded on a Perkin-Elmer Paragon1000 FTIR spectrometer. HRMS were collected with an Agilent1290-micrOTOF Q II (Brucker) spectrometer. Concentrations of metal ions were measured on an Agilent 7500ce inductively coupled plasma mass spectrometer. Absorption and luminescence spectra were studied on a Shimadzu Electronic UV 2100 PC UV-visible spectrophotometer and a Hitachi F-4500 luminescence spectrometer, respectively.

Preparation of IFIC MNPs

The ITCRh6G-Azo/Fe_3O_4@SiO_2-α-CD inclusion complex magnetic nanoparticles (IFIC MNPs) were easily prepared from cyclodextrin-functionalized magnetic silica microspheres (Fe_3O_4@SiO_2-α-CD MNPs) (host) and ITCRh6G-Azo (guest) by a 'self-assembly' technique. The Fe_3O_4@SiO_2-α-CD MNPs were prepared by a multistep process (Scheme 2). In brief, monodisperse superparamagnetic Fe_3O_4@-silica spheres (denoted as Fe_3O_4@SiO_2 MNPs) were prepared using the reported method.[18] Then the cyclodextrin-based silane coupling agent was readily synthesized according to the literature method.[19] α-Cyclodextrin was linked onto the surface of the Fe_3O_4@SiO_2 nanoparticles covalently through the reaction of Fe_3O_4@SiO_2 MNPs and a cyclodextrin-based silane coupling agent (CD-Si) by a grafting reaction.[20,21] The preparation of the ITCRh6G-Azo moiety was described in Scheme 3. All the detailed procedures can be found in the supporting information. The synthetic product was well characterize by FTIR, SEM, XRD, superconducting quantum interference measurement device (SQUID), UV-vis spectroscopy, ^1H NMR and ^{13}C NMR.

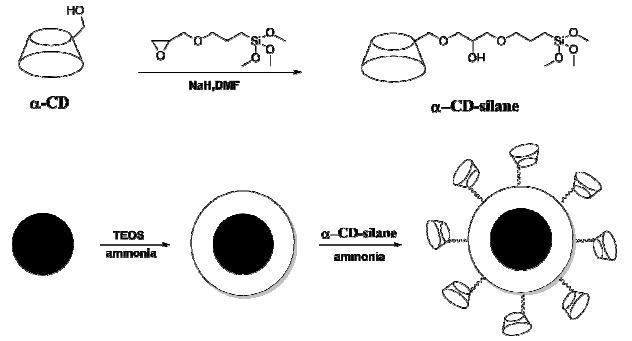

Scheme 2 Preparation of Fe_3O_4@SiO_2-α-CD.

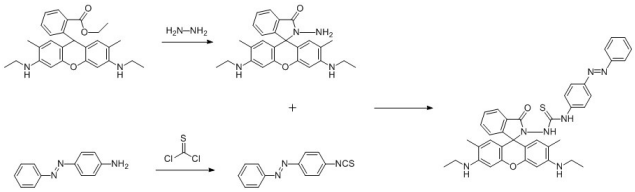

Scheme 3 Synthesis of ITCRh6G-Azo moiety.

Results and discussions

Morphology of the nanoparticles

SEM images show the morphology of the Fe_3O_4 and Fe_3O_4@SiO_2 nanoparticles (Fig 1). Interestingly, it is found that the Fe_3O_4 nanoparticles possess coarse surfaces prepared by a hydrothermal reaction (Fig 1a). While after the coating process, the resulting nanostructures possess a smooth surface and are quite uniform in size (Fig 1b). The diameter of the Fe_3O_4 is 350 nm, the thickness of the SiO_2 shell is 50 nm. In general, we can get a thin SiO_2 layer after the coating process.

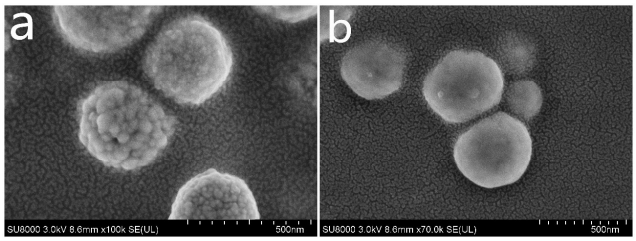

Figure 1 SEM images of Fe_3O_4 (a) and Fe_3O_4@SiO_2 (b).

X-ray powder diffraction pattern analysis

In order to study the crystal structure of the nanoparticles, X-Ray diffraction (XRD) experiments have been carried out (Fig 2). In the figure several strong reflection peaks can be gained in the 2ϑ region of 10^o–80^o. We can index six diffraction peaks from Fig 2 which are (220), (311), (400), (422), (511) and (440), these data are in accordance with the database of magnetite in the JCPDS (JCPDS Card: 19-629) file. This suggested us the retention of crystalline structure after template extraction. Amorphous state SiO_2 shells can be proved to be exist by the broad featureless XRD peak at a low diffraction angle in the XRD pattern of iron-oxide–SiO_2 core–shell nanoparticles. According to the result we can conclude that the Fe_3O_4 MNPs are successfully coated and passivated by the SiO_2 shell.

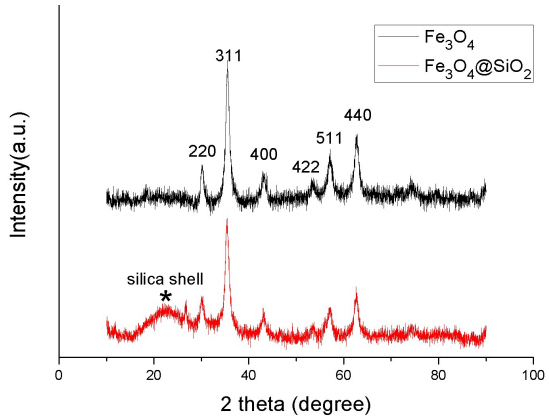

Figure 2 XRD of Fe_3O_4 and Fe_3O_4@SiO_2-α-CD.

Fourier transform IR spectroscopy analysis

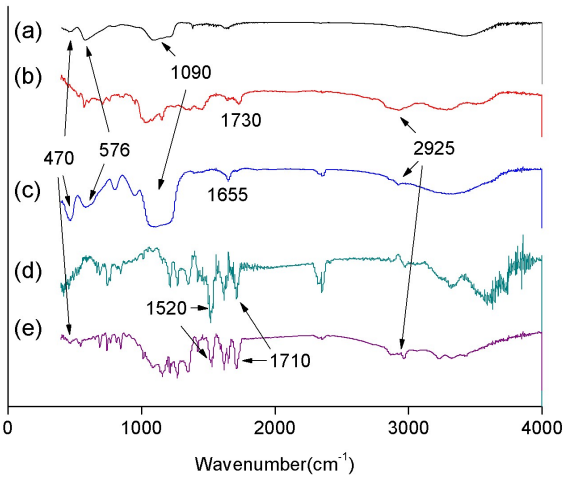

Figure 3 FT-IR spectra of Fe_3O_4@SiO_2 MNPs (a), α-CD (b), Fe_3O_4@SiO_2-α-CD MNPs (c), ITCRh6G-Azo (d) and IFIC MNPs (e).

FTIR was carried out to investigate the bonding information of Fe_3O_4@SiO_2-α-CD MNPs. Fig 3 exhibits the FTIR spectra of Fe_3O_4@SiO_2 MNPs (a), α-CD (b), Fe_3O_4@SiO_2-α-CD MNPs (c), ITCRh6G-Azo (d) and IFIC MNPs moieties (e). Fig 3a and Fig 3c exhibits bands at 470 cm^{-1}, 576 cm^{-1} and 1090 cm^{-1}, which are attributed to bending vibration of Si-O-Si, symmetric Si-O-Si stretching and asymmetric Si-O-Si stretching of silane respectively. The spectrum of Fe_3O_4@SiO_2-α-CD MNPs (c) differs considerably from that of Fe_3O_4@SiO_2 MNPs (a) in the range of 1600-3000 cm^{-1}. Fig 3c exhibits bands at 2925 cm^{-1} and 1655 cm^{-1} , which are attributed to C-H stretching vibration of alkane and O-H bending vibration of cyclodextrin. Especially, the band at 1730 cm^{-1} in Fig 3b shifted to 1655 cm^{-1} in Fig 3c attributed to O-H bending induced by the weaken of hydrogen bond when bonding between silane and cyclodextrin proved the linkage of α-CD and Fe_3O_4@SiO_2 MNPs. Otherwise 1520 cm^{-1} (C-C stretching of benzene skeleton), 1710 cm^{-1}

(C=O stretching vibration) can also be achieved both in Fig 3d and Fig 3e. Based on these data from FT-IR, it can be concluded that the resulting product, ITCRh6G-Azo/Fe_3O_4@SiO_2-α-CD inclusion complex magnetic nanoparticles (IFIC MNPs), was prepared doubtlessly.

Magnetic property

The magnetic hysteresis loops of the Fe_3O_4 and IFIC MNPs measured at T=300K are shown in Fig 4. The low coercivity and no obvious hysteresis indicate the superparamagnetism of the MNPs. The saturation magnetization (Ms) values for Fe_3O_4 nanoparticles and IFIC MNPs were 83.31 and 30.06 $emug^{-1}$, respectively. The nonmagnetic material such as organic ligands and silica shell are the reason for the decrease in Ms. And also the quenching effect is brought by the binding of silica and ITCRh6G-Azo on the particle surface.[22] In addition, the lack of complete coordination of magnetic molecules on the surface increase the surface spin disorientation.[23] A decrease in the effective magnetic moment might have been caused by the disordered structure in the amorphous materials[24]. However, the strong magnetic property has been transmitted from the Fe_3O_4 nanoparticles to IFIC MNPs. When putting a magnet near the bottle contain the IFIC MNPs dispersed CH_3CN-H_2O, the MNPs can be gathered near the magnet within 9 seconds (Fig 5). From the experiment we can conclude that it is promising to offer a simple and efficient way for extracting copper ions from wastewater.

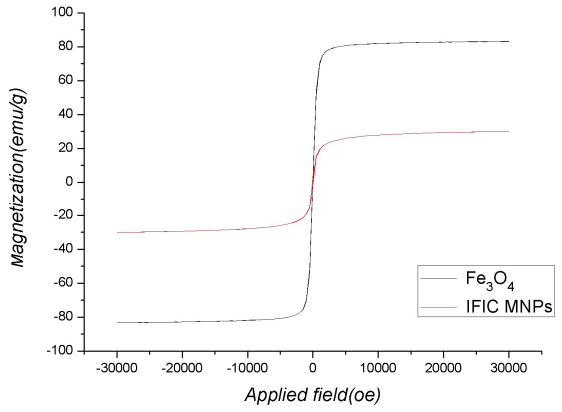

Figure 4 The magnetic hysteresis loops of Fe_3O_4 MNPs (black line) and IFIC MNPs (red line).

Figure 5 Separation of the IFIC MNPs by a magnet near the vessel wall in 9 seconds.

The effect of pH

Protons in the testing solvents can induce great disturbance during the detection of metal ions, so it is essential to investigate the influences of pH values on the detection of Cu^{2+} ions for the chemosensor. A series of experiments were carried out at pH range from 1 to 14 to avoid the precipitation problem caused by $Cu(OH)_2$ under alkaline conditions for Cu^{2+} solutions. The fluorescent spectra of IFIC MNPs were carried out with and without Cu^{2+} ions ([IFIC MNPs]=0.5 g/L, CH_3CN:H_2O=1:1, v/v, excited at 345nm, observed at 555nm), which is shown in Fig 6. When pH < 4, the fluorescence of IFIC MNPs enhanced obviously due to the protonation of the spiral lactam of rhodamine with or without the Cu^{2+} ions. When pH>12, the fluorescence recedes with the existence of Cu^{2+} ions (black line) and retains without Cu^{2+} due to the conformation of $Cu(OH)_2$ under alkaline conditions. When the pH value range from 7 to 12, the intensity of fluorescence remains unchanged. Therefore the testing solvent is buffered at 7.20.

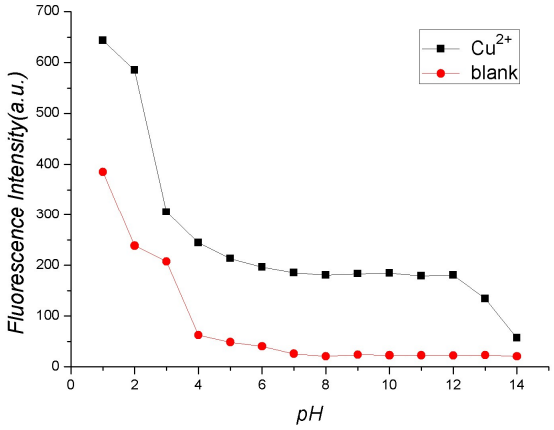

Figure 6 Fluorescence intensity of IFIC MNPs in CH_3CN-H_2O (1/1, v/v) with and without Cu^{2+} ions measured as a function of pH.

Fluorescence and UV-vis spectrum properties

Fluorescence spectra and UV-vis absorption spectra were conducted to gain insight into the signaling properties of the IFIC MNPs toward Cu^{2+}. The fluorescence spectra of the Cu^{2+} ions was carried out using a solution of IFIC MNPs (0.5g L^{-1}) in buffered (0.05M Tris-HCl, pH=7.20) CH_3CN-H_2O (1/1, v/v). The fluorescence spectra of different concentrations of Cu^{2+} ions in IFIC MNPs solution are shown in Fig 7. Upon addition of increasing concentrations of Cu^{2+} ions (0 to 1.0×10^{-5} mol L^{-1}), a significant enhancement of the characteristic fluorescence of the rhodamine 6G fluorophore moiety in a Cu^{2+} ion concentration-dependent way emerges at 555nm (excited at 345nm), accompanied by an obvious yellow-green fluorescence enhancement. A linear relationship existed between the fluorescence intensity of IFIC MNPs and concentration of Cu^{2+} over the range 5.0×10^{-6} to 1.0×10^{-5} mol L^{-1}. The correlation coefficient was R=0.99835, SD=0.97743, k=11.72817. The detection limit, based on the definition by IUPAC,[25] was 2.5×10^{-7} mol L^{-1} (CDL=3SD k^{-1}). This value is lower than the acceptable value mandated by the EPA for the concentration of copper in drinking water (0.5mg L^{-1}).[26] Thus, the sensor can be useful in detecting inorganic copper in

samples of biological products, drugs, fish and other aqueous solutions.

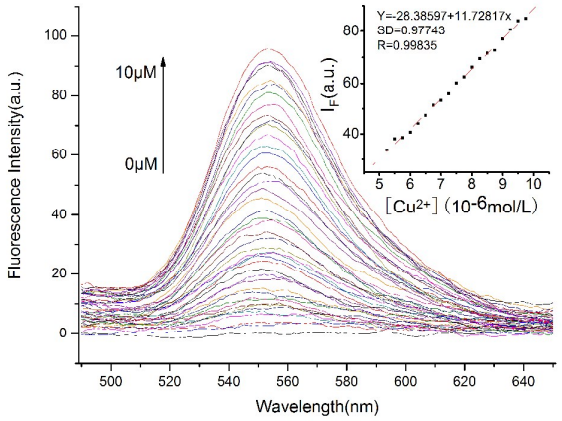

Figure 7 Fluorescent spectra of IFIC MNPs (0.5g L^{-1}) in the absence and presence of Cu^{2+} (0 to 1.0×10^{-5} mol L^{-1}). The inset shows fluorescent intensity as a function of Cu^{2+} concentration (CH_3CN-H_2O, 1:1, v/v, buffered at pH 7.20 with 0.05M Tris-HCl, excitated at 345nm, monitored at 555nm).

The UV-vis absorption spectra of the IFIC MNPs with varying Cu^{2+} concentrations were recorded, as shown in Fig 8. Upon addition of Cu^{2+} to SFIC MNPs (0.5g L^{-1}), the peak around 528nm is significantly enhanced, suggesting the formation of the ring-opened tautomer of the rhodamine 6G moiety upon Cu^{2+} binding. According to the molecular structure and spectral results of the ITCRh6G-Azo moiety, it is concluded that the Cu^{2+} ions could chelate with the carbonyl O and thiourea S atoms and thus a ring opening of the spirolactam of rhodamine 6G took place. The hydrazine modified rhodamine is just suitable for the Cu^{2+} ions in the aspect of steric effect, so this reaction has a high selectivity for Cu^{2+} ions. In this case, the solution exhibited an obvious and characteristic color change from light yellow to pink. IFIC MNPs thus can be used as a "naked eye" detector of Cu^{2+}. The detection threshold for Cu^{2+} ranged from 0 to 5.0×10^{-5} mol L^{-1}, and at this level the color change was very obvious.

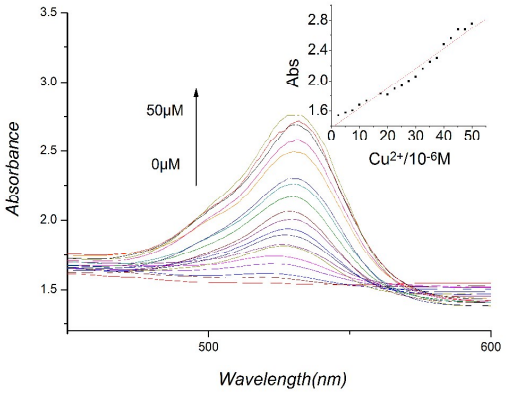

Figure 8 UV-vis spectra of the IFIC MNPs (0.5g L^{-1}). The inset shows absorbance intensity as a function of Cu^{2+} concentration (0 to 5.0×10^{-5} mol L^{-1}). (CH_3CN-H_2O, 1:1, v/v, buffered at pH = 7.20 with 0.05M Tris-HCl, monitored at 528nm).

Metal ion competition studies

The fluorescence emission responses of IFIC MNPs upon addition of various biologically and environmentally relevant metal ions, including Zn^{2+}, Co^{2+}, Ba^{2+}, Mn^{2+}, K^{+}, Ca^{2+}, Ni^{2+}, Mg^{2+}, Hg^{2+}, Pb^{2+}, Fe^{3+} and Cd^{2+} ions, each with a concentration of 10μM (white bars in Fig 9) were carried out to estimate the selectivity of IFIC MNPs as a fluorescence probe for Cu^{2+} ions (monitored at 555nm, excited at 345nm),. As we expected, besides the weak effect brought by Hg^{2+}, the above-mentioned metal ions show little effect on the fluorescence intensity of the nanosensor. However, compared with the marked enhancement provoked by Cu^{2+} ions (5μM), the influence of the above-mentioned metal ions is negligible.

To test the practical applications of IFIC as a Cu^{2+} (monitored at 555nm, excited at 345nm) selective fluorescence sensor, competition experiments were carried out to investigate the effect of other coexisting cations with Cu^{2+} in the presence of IFIC. The emission spectra containing IFIC (0.5g L^{-1}) and Zn^{2+}, Co^{2+}, Ba^{2+}, Mn^{2+}, K^{+}, Ca^{2+}, Ni^{2+}, Mg^{2+}, Hg^{2+}, Pb^{2+}, Fe^{3+}, Cd^{2+} (10μm) followed by addition of Cu^{2+} (5μm) were recorded (black bars in Fig 9). No obvious interference were shown by those ions in the detection for Cu^{2+}. Thus, the IFIC MNPs exhibited excellent selectivity toward Cu^{2+}, which makes their practical application feasible.

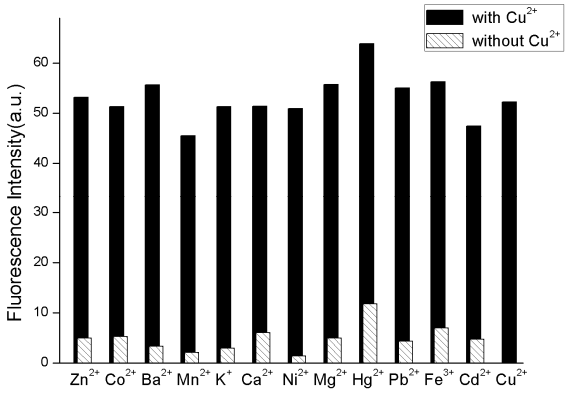

Figure 9 White bars: fluorescence emission response of IFIC MNPs (0.5g L^{-1}) in the presence of different metal ions (1.0×10^{-5} mol L^{-1}) in CH_3CN–H_2O solution. Black bars: fluorescence emission response of IFIC MNPs upon addition of 5.0×10^{-6} mol L^{-1} Cu^{2+} ions in the presence of 1.0×10^{-5} mol L^{-1} of each of background metal ions (CH_3CN–H_2O, 1 : 1, v/v, buffered at pH 7.20 with 0.05M Tris-HCl, monitored at 555 nm, excited at 345nm).

Adsorption experiments of metal ions onto IFIC MNPs.

Adsorption kinetic experiments were carried out to investigate the adsorption ability of IFIC MNPs for Cu^{2+} and other metal ions in the solutions (Fig 10). The IFIC MNPs were added to aqueous solutions containing Cu^{2+} ions from 0 to 50mg/L ([IFIC MNPs]=5g/L, CH_3CN-H_2O=1:1, v/v, pH=7.20, 0.05M Tris-HCl).

Using a magnet to remove the magnetic nanoparticles from the solvent after 24 hours and ICP-MS to detect the concentration of Cu^{2+} in the solvent. Fig 10a shows the equilibrium adsorption amounts within 24 hours under various equilibrium concentrations. It was found from Fig 10a that the adsorption of Cu^{2+} increased with the augment of [Cu^{2+}] and after 15mg/L the value remained unchanged. The initial increase of adsorption may due to the vast coordination sites on the surface of IFIC MNPs, when all the sites were occupied the value leveled off. The Langmuir adsorption equation was applied to analyze the data which is given as: $C_e/q_e = 1/K_Lq_m + C_e/q_m$. where q_e is the equilibrium quantity of the metals ions adsorbed onto the SFIC MNPs (mg g^{-1}), C_e is the equilibrium concentration (mg L^{-1}), and q_m (mg g^{-1}) and K_L (L mg^{-1}) are the Langmuir constants related to the saturation adsorption capacity and binding energy (affinity), respectively. The Langmuir C_e/q_e versus C_e plot was shown in Fig 10b and the equation was calculated as C_e/q_e = 0.16633+ 0.05489C_e. And after calculation we can get that q_m = 18.22mg/g, K_L = 0.33L/mg, R^2=0.9597, which are also shown in Table 1.

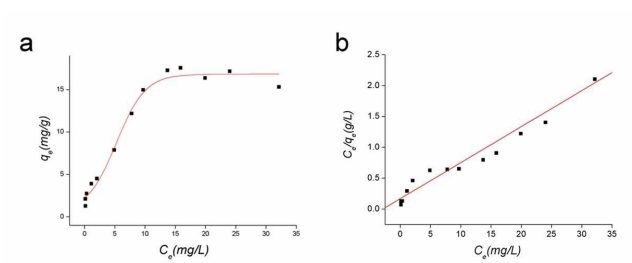

Figure 10 Adsorption isotherm (a) and Langmuir plot of Cu^{2+} (b) on the IFIC MNPs.

Table 1 The Langmuir constants for Cu^{2+} on the IFIC MNPs.

Metal ion	K_L / L mg^{-1}	q_m / mg g^{-1}	R^2
Cu^{2+}	0.33	18.22	0.9597

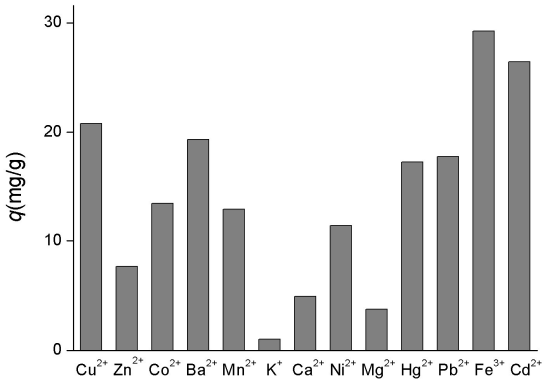

Figure 11 Adsorption capacity of IFIC MNPs for various metal ions. (CH_3CN–H_2O, 1 : 1, v/v, buffered at pH 7.20 with 0.05M Tris-HCl, [Cu^{2+}]=1.0×10^{-5} mol L^{-1}, metal ions: 100mg L^{-1}, MNPs: 2g L^{-1})

Adsorption experiments were also carried out for other metal ions such as Zn^{2+}, Co^{2+}, Ba^{2+}, Mn^{2+}, K^+, Ca^{2+}, Ni^{2+}, Mg^{2+}, Hg^{2+}, Pb^{2+}, Fe^{3+}, Cd^{2+}, each with the concentration of 100mg/L ([IFIC MNPs]=2g/L, [Cu^{2+}]=1.0×10^{-5} mol L^{-1}, CH_3CN-H_2O=1:1, v/v, pH=7.20, 0.05M Tris-HCl). Fig 11 shows the adsorption amounts of each metal ion. The results showed us that the IFIC MNPs can adsorb metal ions to an extent and can even reach to 28mg/g for Fe^{3+}. From the results we can conclude that the IFIC MNPs shows great adsorptivity to different metal ions which may due to the intensive distribution of α-cyclodextrin on the surface of IFIC MNPs. The ability of adsorption endowed the MNPs a promising prospect for the recycling of metal ions in solutions.

Regeneration efficiency of the sensing system

Recycling of the IFIC nanoparticles was conducted for detection of copper ions (Fig 12). After each cycle, EDTA was added into the testing solvent to bind Cu^{2+} in order to make the complex dissociate. After magnetic separation, IFIC nanoparticles were washed in ultrasonic with DMF at 50°C, this procedure can destroy the self-assembled structure, magnetically separated again, dried under vacuum, and reused in the system of solution of ITCRh6G-Azo moieties to rebuild the host-guest moiety. The recycling was easy and high yielding. Fig 12. illustrates the fluorescent intensity of the IFIC–Cu^{2+} in each cycle ([Cu^{2+}]=1.0×10^{-5} mol L^{-1}). After 5 cycles, the ability to detect the Cu^{2+} ion is still active and efficient. Through this procedure, we can recycle the dye molecule and the magnetic nanoparticles, these can be reused in the next experiment or testing, this recyclable feature can't be achieved in those covalent bonding testing system for metal ions.

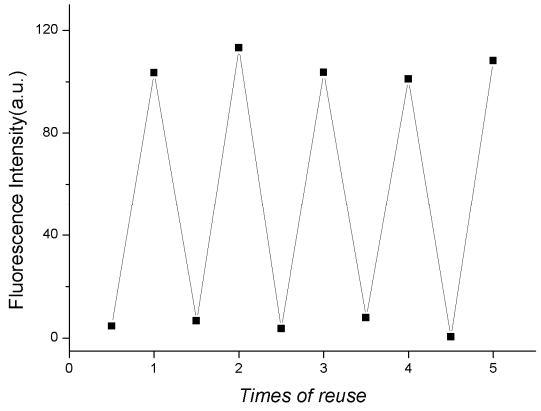

Figure 12 Recycling and reuse of the IFIC MNP sensors for Cu^{2+}. (CH_3CN–H_2O, 1 : 1, v/v, buffered at pH 7.20 with 0.05M Tris-HCl, [Cu^{2+}]=1.0×10^{-5} mol L^{-1}, at 555nm).

Conclusions

In conclusion, a new type of fluorescent chemosensor for sensing and separating Cu^{2+} efficiently in aqueous solution has been prepared. It has a core-shell Fe_3O_4@SiO_2-α-CD structure loaded with ITCRh6G-Azo moiety *via* host-guest interaction. These multifunctional nanoparticles exhibit a high selectivity

and an excellent high sensitivity for targeting copper ions over a number of other metal ions tested, with the detection limit found to be 2.5×10^{-7} mol L^{-1}. Furthermore, the recycling of the IFIC nanoparticles is easy and high-yielding and the described approach (based on grafting reaction and self-assembly techniques) is simple and effective. It proved to be a promising alternative for developing high-performance fluorescent sensing materials for copper ions detection in aqueous solution with both high sensitivity and selectivity.

Acknowledgements

We thank the National Natural Science Foundation of China (no.21174052), the Natural Science Foundation of Jilin Province of China (no. 20130101024JC) and Jilin Provincial Science &Technology Department (no. 20140204054GX) for their generous financial support.

Notes and references

1 S. P. Wu, R. Y. Huang and K. J. Du, *Dalton Trans*, 2009, 4735-4740.
2 R. Krämer, *Angew. Chem. Int. Ed.*, 1998, **37**, 772-773.
3 C. Deraeve, C. Boldron, A. Maraval, H. Mazarguil, H. Gornitzka, L. Vendier, M. Pitie and B. Meunier, *Chem. Eur. J.*, 2008, **14**, 682-696.
4 B. L. Ma, S. Z. Wu and F. Zeng, *Sens. Actuators. B.*, 2010, **145**, 451-456.
5 Z. J. Chen, L. M. Wang, G. Zou, J. Tang, X. F. Cai, M. S. Teng and L. Chen, *Spectrochim. Acta. A.*, 2013, **105**, 57-61.
6 Y. Xiang, A. J. Tong, P. Y. Jin and Y. Ju, *Org. Lett.*, 2006, **8**, 2863-2866.
7 M. Dong, T. H. Ma, A. J. Zhang, Y. M. Dong, Y. W. Wang and Y. Peng, *Dyes. Pigments.*, 2010, **87**, 164-172.
8 Y. Ma, B. Z. Zheng, Y. Zhao, H. Y. Yuan, Y. Q. Cai, J. Du and D. Xiao, *Biosens. Bioelectron.*, 2013, **48**, 138-144.
9 Q. He, E. W. Miller, A. P. Wong and C. J. Chang, *J. Am. Chem. Soc.*, 2006, **128**, 9316-9317.
10 J. H. Jung, J. H. Lee and S. Shinkai, *Chem. Soc. Rev.*, 2011, **40**, 4464-4474.
11 C. Wang, S. Tao, W. Wei, C. Meng, F. Liua and M. Hana, *J. Mater. Chem.*, 2010, **20**, 4635-4641.
12 N. Insin, J. B. Tracy, H. Lee, J. P. Zimmer, R. M. Westervelt, M. G. Bawendi, R. M. Westervelt and M. G. Bawendi, *ACS Nano.*, 2008, **2**, 197-202.
13 R. Hao, R. J. Xing, Z. C. Xu, Y. L. Hou, S. Gao and S. H. Sun, *Adv. Mater.*, 2010, **22**, 2729-2742.
14 J. S. Yang and T. Swager, *J. Am. Chem. Soc.*, 1998, **120**, 5321-5322.
15 D. R. Bae, W. S. Han, J. M. Lim, S. W. Kang, J. Y. Lee, D. M. Kang and J. H. Jung, *Langmuir.*, 2010, **26**, 2181-2185.
16 H. J. Kim, M. Lee, H. L. Mutihac, J. Vicens and J. S. Kim, *Chem. Soc. Rev.*, 2012, **41**, 1173-1190.
17 R. A. Potyrailo, R. C. Conrad, A. D. Ellington and G. M. Hieftje, *Anal. Chem.*, 1998, **70**, 3419-3425.
18 S. Wang, Q. W. Liu, Y. Zhang, S. D. Wang, Y. X. Li, Q. B. Yang and Y. Song, *Appl. Surf. Sci.*, 2013, **279**, 150-158.
19 X. Xu, C. Deng, M. Gao, W. Yu, P. Yang and X. Zhang, *Adv. Mater.*, 2006, **18**, 3289-3293.
20 X. Y. Ling, I. Y. Phang, G. J. Vancso, J. Huskens and D. N. Reinhoudt, *Langmuir.*, 2009, **25**, 3260-3263.
21 D. Zhang and J. Chang, *Adv. Mater.*, 2007, **19**, 3664-3667.
22 S. Ghosh, A. Z. M. Badruddoza, M. S. Uddin and K. Hidajat, *J. Colloid. Interface. Sci.*, 2011, **354**, 483-492.
23 D. H. Chen and S. H. Wu, *Chem. Mater.*, 2000, **12**, 1354-1360.
24 R. H. Kodama, A. E. Berkowitz, E. J. McNiff and S. Foner, *J. Appl. Phys.*, 1997, **81**, 5552-5557.
25 H. M. N. H. Irving, H. Freiser and T. S. West, *IUPAC Compendium of Analytical Nomenclature, Definitive Rules*, Pergamon Press, Oxford, 1981.
26 *Guidelines for Drinking-Water Quality; World Health Organization: Geneva*, 1996.

Graphical abstract